

## Crystal Structure and Vibrational Studies of Glycine-LiNO<sub>3</sub> and Glycine-NaNO<sub>3</sub> Crystals\*

by J. Baran<sup>\*\*</sup>, M. Drozd, A. Pietraszko, M. Trzebiatowska and H. Ratajczak

*Institute of Low Temperature and Structure Research, Polish Academy of Sciences,  
P.O. Box 1410, 50950 Wrocław 3, Poland*

*(Received April 27th, 2003; revised manuscript July 3rd, 2003)*

New crystal of glycine with lithium nitrate  $[(\text{NN}_3^+\text{CH}_2\text{COO}^-)\text{LiNO}_3]$ ; GLiN was discovered. It belongs to the space group  $\overline{\text{P}1}$  of the triclinic system. Its structure is different from that of the glycine-NaNO<sub>3</sub> crystal (GNaN). The Li<sub>2</sub>O<sub>6</sub> units can be distinguished in the GLiN crystal. They have a shape of two symmetry related (through a centre of inversion) tetrahedrons with a common edge. Powder IR and FT-Raman spectra of GLiN and its deuterated analogue and of GNan were measured and discussed with respect to the crystal structures. The splitting of some vibrations is observed, which suggests the breaking of the selection rules for the centre of inversion.

**Key words:** glycine-LiNO<sub>3</sub>, glycine-NaNO<sub>3</sub>, X-ray crystal structure, IR, Raman, hydrogen bond, phase transition

Some complexes of the amino acids with simple inorganic salts may exhibit ferroelectrics properties. Pepinsky, Okaya, Eastman and Mitsui [1] discovered that glycine silver(I) nitrate (abbreviated hereafter as GSN) was ferroelectrics below  $-55^\circ\text{C}$ . Ferroelectricity was also discovered for diglycine manganese chloride ( $T_c = +55^\circ\text{C}$ ) [2] and for trissarcosine calcium chloride [3]. Some crystals of the amino acids with simple inorganic salts appear to be promising materials for optical second harmonic generation (SHG). Very recently, it was discovered that a crystal of glycine sodium nitrate exhibited SHG two times higher than that of the KDP [4]. According to our best knowledge, there is no information on other crystal of glycine with lithium, potassium, rubidium and caesium nitrates, respectively. Therefore, we have undertaken such research. We found that such complex was formed only with lithium nitrate. The crystal structure of the glycine lithium nitrate (abbreviated hereafter as GLiN) and its vibrational properties are the subject of this paper. Additionally, the vibrational spectra of the glycine sodium nitrate (abbreviated hereafter as GNan) are also presented and discussed with respect to its structure.

\* Dedicated to Prof. M. Szafran on the occasion of his 70th birthday.

\*\* Corresponding author. E-mail address: baran@int.pan.wroc.pl (J. Baran).

## EXPERIMENTAL.

The aqueous solutions containing glycine and  $MNO_3$  ( $M = Li, Na, K, Rb, Cs$ ) in the ratio 1:1 were prepared and evaporated at ambient temperature. The crystals of glycine- $LiNO_3$  (GLiN) and glycine- $NaNO_3$  (GNaN) complexes were obtained only. The deuterated sample of GLiN was prepared by fourfold recrystallization from  $D_2O$ .

The X-ray study was performed on KM-4 single crystal diffractometer with the CCD detector. The structure was solved and refined using SHELX-97 program [5]. The crystal data and refinement parameters of the studied crystal are listed in Table 1.

**Table 1.** Crystal data and structure refinement for glycine lithium nitrate  $[(NH_3CH_2COO)LiNO_3]$ .

Empirical formula	$C_2H_5LiN_2O_5$		
Formula weight	144.02		
Temperature	293(2) K		
Wavelength	0.71073 Å		
Crystal system, space group	Triclinic, $P\bar{1}$		
Unit cell dimensions	$a = 5.5900(10)$ Å	$\alpha = 92.13(3)$ deg.	
	$b = 5.8980(10)$ Å	$\beta = 92.79(3)$ deg.	
	$c = 8.658(2)$ Å	$\gamma = 97.09(3)$ deg.	
Volume	282.67(10) Å <sup>3</sup>		
Z, Calculated density	2, 1.692 Mg/m <sup>3</sup>		
Absorption coefficient	0.163 mm <sup>-1</sup>		
$F(000)$	148		
Crystal size	0.34 × 0.32 × 0.31 mm		
Theta range for data collection	3.68 to 36.32 deg.		
Index ranges	-6<=h<=9, -7<=k<=7, -14<=l<=12		
Reflections collected / unique	3591 / 1951 [R(int) = 0.0249]		
Completeness to 2theta = 30.00	87.7%		
Refinement method	Full-matrix least-squares on $F^2$		
Data / restraints / parameters	1951 / 0 / 112		
Goodness-of-fit on $F^2$	0.960		
Final R indices [ $I > 2\sigma(I)$ ]	R1 = 0.0330, wR2 = 0.0817		
R indices (all data)	R1 = 0.0418, wR2 = 0.0849		
Extinction coefficient	0.749(15)		
Largest diff. peak and hole	0.397 and -0.246 e.Å <sup>-3</sup>		

The infrared and Raman spectra were measured with a Bruker IFS-88 spectrometer equipped with FRA-106 attachment for the FT-Raman. The spectra were measured with resolution 2 cm<sup>-1</sup> and weak apodisation. The IR spectra were measured for emulsions in Nujol and Fluorolube.

The differential scanning calorimetric measurements were performed with a Perkin-Elmer DSC-7 equipped with low temperature CCA-7 attachment. The scanning ratio was 20 K/min. The sample weight was *ca.* 20 mg.

## RESULTS AND DISCUSSION

**The DSC results:** The crystal of the GLiN does not show any phase transition in the temperature region between 394 and 100 K. At *ca.* 394 K the crystal undergoes decomposition.

**The crystal structure:** The atomic parameters are listed in Table 2. The interatomic distances and interbond angles are listed in Table 3. The parameters of the hydrogen bonds are listed in Table 4. The views of the crystal structure towards  $(51\bar{3})$  and  $(\bar{1}6\bar{2})$  planes are shown in Figures 1 and 2.

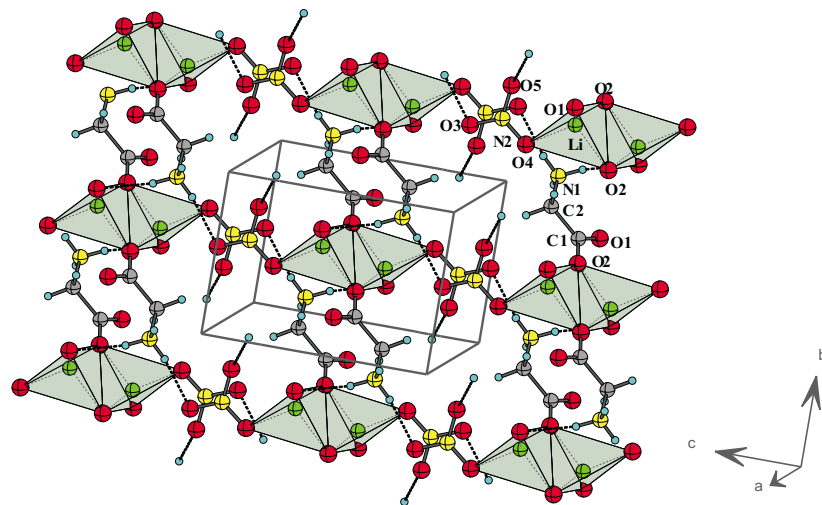


**Figure 1.** The view of the structure towards the  $(51\bar{3})$  plane for the GLiN crystal.

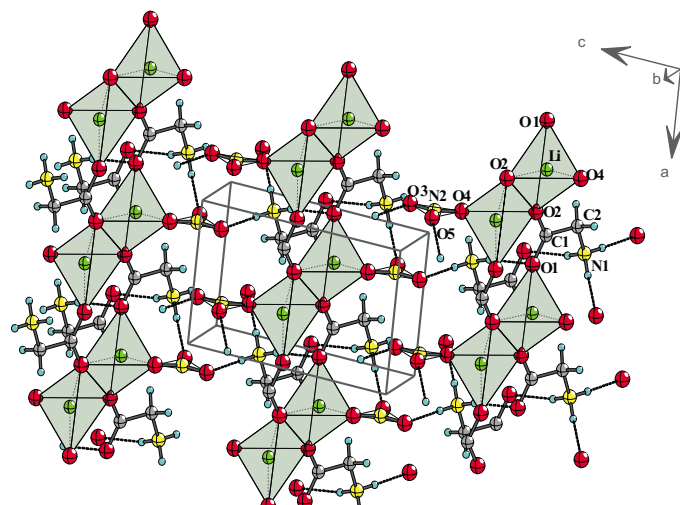


**Figure 2.** The view of the structure towards  $(\bar{1}6\bar{2})$  plane for the GLiN crystal.

**Table 2.** Atomic coordinates ( $\times 10^4$ ) and equivalent isotropic displacement parameters ( $\text{\AA}^2 \times 10^3$ ) for glycine lithium nitrate  $[(\text{NH}_3\text{CH}_2\text{COO})\text{LiNO}_3]$ . U(eq) is defined as one third of the trace of the orthogonally normalized Uij tensor.

	x	y	z	U (eq)
O(1)	43(1)	7587(1)	5554(1)	23(1)
O(2)	3816(1)	6742(1)	5562(1)	29(1)
C(1)	2209(1)	7859(1)	6039(1)	18(1)
C(2)	3005(1)	9710(1)	7286(1)	24(1)
N(1)	1046(1)	11111(1)	7593(1)	26(1)
N(2)	-2515(1)	5534(1)	9116(1)	23(1)
O(3)	-2465(1)	4810(1)	10442(1)	30(1)
O(4)	-2722(1)	4171(1)	7955(1)	35(1)
O(5)	-2369(1)	7635(1)	8929(1)	37(1)
Li	-2973(2)	5820(2)	6020(1)	26(1)
H(1)	4314(14)	10759(13)	6977(8)	44(2)
H(2)	3428(13)	9003(13)	8208(9)	42(2)
H(3)	1531(13)	12273(13)	8285(9)	44(2)
H(4)	-217(14)	10241(14)	7980(9)	49(2)
H(5)	527(14)	11631(14)	6703(9)	47(2)

**Table 3.** Bond lengths [ $\text{\AA}$ ] and angles [deg] for glycine lithium nitrate  $[(\text{NH}_3\text{CH}_2\text{COO})\text{LiNO}_3]$  and for glycine sodium nitrate  $[(\text{NH}_3\text{CH}_2\text{COO})\text{NaNO}_3]$  [6].

Glycine molecule	GLiNO <sub>3</sub>	GNaNO <sub>3</sub> [6]
O(1)–C(1)	1.2511(6)	1.242(26)
O(2)–C(1)	1.2540(7)	1.247(21)
C(1)–C(2)	1.5169(8)	1.520(40)
C(2)–N(1)	1.4791(8)	1.480(26)
C(2)–H(1)	0.953(7)	0.97(1)
C(2)–H(2)	0.948(8)	0.97(1)
N(1)–H(3)	0.899(8)	0.890(3)
N(1)–H(4)	0.906(8)	0.890(3)
N(1)–H(5)	0.889(8)	0.890(3)
O(1)–C(1)–O(2)	125.37(5)	126.03(31)
O(1)–C(1)–C(2)	118.26(5)	117.76(25)
O(2)–C(1)–C(2)	116.36(4)	116.19(26)
N(1)–C(2)–C(1)	111.24(4)	111.92(25)
N(1)–C(2)–H(1)	105.4(5)	109.22(28)
C(1)–C(2)–H(1)	111.7(4)	109.25(29)
N(1)–C(2)–H(2)	108.8(5)	109.18(28)
C(1)–C(2)–H(2)	108.5(4)	109.21(28)
H(1)–C(2)–H(2)	111.2(6)	107.97(32)
C(2)–N(1)–H(3)	111.9(5)	109.49(25)
C(2)–N(1)–H(4)	110.2(5)	109.48(25)
H(3)–N(1)–H(4)	107.6(7)	109.46(27)
C(2)–N(1)–H(5)	108.6(5)	109.55(25)
H(3)–N(1)–H(5)	110.8(7)	109.41(29)
H(4)–N(1)–H(5)	107.5(7)	109.43(31)
O(1)–C(1)–C(2)–N(1)	-6.90(6)	
O(2)–C(1)–C(2)–N(1)	172.05(4)	
Nitrate ion		
N(2)–O(3)	1.2397(6)	1.247(5)
N(2)–O(5)	1.2493(7)	1.235(4)
N(2)–O(4)	1.2556(7)	1.241(5)
O(3)–N(2)–O(5)	119.92(5)	120.47(24)
O(3)–N(2)–O(4)	120.60(5)	119.07(26)
O(5)–N(2)–O(4)	119.48(5)	120.46(26)

Table 3 (continuation)

<b>Lithium contacts</b>	
Li–O(2 <sup>#3</sup> )	1.9655(11)
Li–O(2 <sup>#2</sup> )	1.9974(12)
Li–O(1)	1.9380(11)
Li–O(4)	1.9754(12)
O(2)–Li <sup>#1</sup>	1.9655(12)
O(2)–Li <sup>#2</sup>	1.9974(8)
O(2)–O(2 <sup>#3</sup> )	2.7520(19)
Li–Li <sup>#4</sup>	2.8517(5)
O(1)–Li–O(2 <sup>#3</sup> )	124.57(5)
O(1)–Li–O(4)	112.78(5)
O(2 <sup>#3</sup> )–Li–O(4)	113.84(5)
O(1)–Li–O(2 <sup>#2</sup> )	109.73(5)
O(2 <sup>#3</sup> )–Li–O(2 <sup>#2</sup> )	87.96(5)
O(4)–Li–O(2 <sup>#2</sup> )	102.14(5)
O(1)–Li–Li <sup>#4</sup>	128.87(6)
O(2 <sup>#3</sup> )–Li–Li <sup>#4</sup>	44.43(3)
O(4)–Li–Li <sup>#4</sup>	115.21(6)
O(2 <sup>#2</sup> )–Li–Li <sup>#4</sup>	43.54(3)

Symmetry transformations used to generate equivalent atoms:

#1 x+1,y,z #2 -x,-y+1,-z+1 #3 x-1,y,z #4 -x-1,-y+1,-z+1

**Table 4.** Hydrogen-bond geometry parameters [Å and deg.] for glycine lithium nitrate  $[(\text{NH}_3\text{CH}_2\text{COO})\text{LiNO}_3]$ .

D–H···A	d(D–H)	d(H···A)	d(D···A)	∠(DHA)
N(1)–H(3)···O(3 <sup>#5</sup> )	0.899(8)	2.007(8)	2.8986(11)	170.8(7)
N(1)–H(3)···O(5 <sup>#5</sup> )	0.899(8)	2.432(7)	3.1050(10)	131.8(6)
N(1)–H(4)···O(5)	0.906(8)	2.054(8)	2.9343(11)	163.7(8)
N(1)–H(5)···O(1 <sup>#6</sup> )	0.889(8)	2.043(8)	2.9147(10)	166.3(8)
C(2)–H(2)···O(3 <sup>#1</sup> )	0.948(8)	2.583(8)	3.3643(10)	139.9(6)
C(2)–H(1)···O(4 <sup>#7</sup> )	0.954(8)	2.535(8)	3.3416(10)	142.4(6)

Symmetry transformations used to generate equivalent atoms:

#1 -x, -y+1,-z+2 #5 -x,-y+2,-z+2 #6 -x,-y+2,-z+1 #7 x+1, y+1,z

The structure of the GLiN crystal is different from its sodium analogue [6]. In the crystals of GNan the layers of the nitrate ions alternate with the layers of glycine molecules. In the GLiN crystal the  $\text{Li}^+$  cations are tetrahedrally surrounded by four oxygen atoms (see Table 3). Three contacts are made to the oxygen atoms (O(2<sup>#3</sup>), O(2<sup>#2</sup>) and O(1)) of the glycine molecules. The fourth contact (1.9754(12) Å) is made to the O(4) atom of the nitrate ion. There is a direct contact between two lithium cations related by the centre of inversion. The distance between those cations is equal to 2.8517(19) Å, which is considerably longer than the sum of their crystal ionic radii ( $2 \times 0.68 = 1.36$  Å). Each O(2) atom forms two contacts (1.9655(11) and 1.9974(12) Å) with lithium cations (Li and Li<sup>#4</sup>) related to each other by the centre of inversion. Thus, the O(2) atom belongs to tetrahedrons of two lithium atoms. In such a way double tetrahedrons ( $\text{Li}_2\text{O}_6$ ) with a common edge are formed. The common edge (2.7520(8) Å) is made by the O(2<sup>#3</sup>) and O(2<sup>#2</sup>) atoms. The double tetrahedrons  $\text{Li}_2\text{O}_6$

seem to be the most important structural element in the GLiN crystal. The neighbouring double tetrahedrons (shifted by the  $\mathbf{a}$  distance) are joined together by the carboxylic groups of two glycine zwitterions related by the centre of inversion at  $0, \frac{1}{2}, \frac{1}{2}$ .

Each glycine molecule forms hydrogen bond by the N(1)–H(4) group with the O(5) atom of the nitrate ion (N(1)H(4)…O(5); 2.9343(11) Å). The H(3) atom of the amine group is involved in the bifurcated hydrogen bond with the O(5<sup>#5</sup>) and O(3<sup>#5</sup>) oxygen atoms of the other (related to the previous one by the centre of inversion) nitrate ion. The N–H(5)…O(1<sup>#6</sup>) hydrogen bonds join the glycine zwitterions into centrosymmetric dimers. There are no direct hydrogen bonds between these dimers.

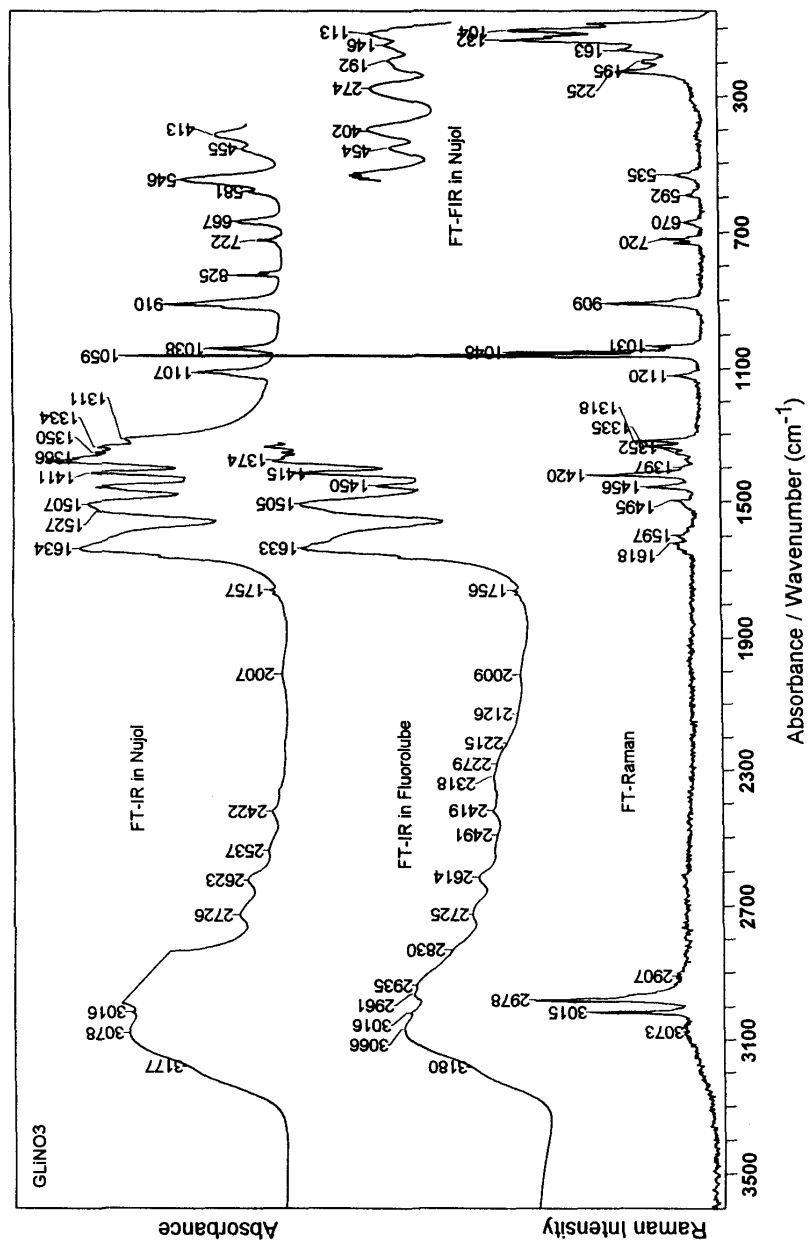
The glycine molecules existing in the zwitterionic form are not flat. The N(1) atom is deviated by 0.2153(8) Å and atom C(2) by 0.0271(8) Å from the plane of the carboxylic group. The angle between the plane of the carboxylic group and CCN skeleton is 7.5°. The angle between the CCOO plane and the C(2)–N(1) bonds is 8.37(1)°. This angle is smaller than those observed in the  $\alpha$ -glycine (18.6(3)°),  $\beta$ -glycine (24.8(3)°) and  $\gamma$ -glycine (12.7(2)°) crystals [7]. The O(1) and O(2) atoms are out of the CCN plane by (1.1324(8) Å) and (–1.5550(9) Å), respectively. The interatomic distances and interbond angles (see Table 3) are very similar to those observed in  $\alpha$ -,  $\beta$ - and  $\gamma$ -form of the glycine [7] and in the case of GNan [6]. The two C–H bonds are very similar in the GLiN crystal (0.948(8) and 0.954(8) Å). Both these protons are engaged in the hydrogen bonds with O(5) and O(4) oxygen atoms of the nitrate ions. These hydrogen bonds (C(2)–H(2)…O(3<sup>#1</sup>); 3.3643(10) Å; C(2)–H(1)…O(4<sup>#7</sup>), 3.3416(10) Å) seem to be similar (see Table 4). In fact, their C…O distances are different. However, for the C(2)–H(2)…O(3<sup>#1</sup>) hydrogen bond, with shorter C…O distance (3.3643(10) Å), the C–H…O angle is smaller (139.9(6)°) than that (142.4(6)°) in the case of the C(2)–H(1)…O(4<sup>#7</sup>) hydrogen bond with longer C…O distance (3.3416(10) Å).

The nitrate ions are almost planar. Nevertheless, the nitrogen atom is shifted by 0.0015 Å out of the plane formed by the oxygen atoms. The N(2)–O distances are between 1.2397(6) Å (N(2)–O(3)) and 1.2556(7) Å. The longest N–O bond (1.2556(7) Å) appears to be the N(2)–O(4), whose O(4) oxygen atom is in direct contact with the Li<sup>+</sup> cation only. The oxygen atom of the intermediate bond (N(2)–O(5), (1.2493(7) Å) is involved in two (N(1)–H(4)…O(5) and N(1<sup>#5</sup>)–H(3<sup>#5</sup>)…O(5)) hydrogen bonds.

### The vibrational studies.

**Selection rules:** The glycine molecules and nitrate ions occupy C<sub>1</sub> sites. The formal classification of the fundamental modes predicts 24 A<sub>g</sub> + 24 A<sub>u</sub> modes for the internal vibrations of the glycine, 6A<sub>g</sub> + 6A<sub>u</sub> modes for the internal vibrations of the nitrate ions, 9A<sub>g</sub> + 6 A<sub>u</sub> translational modes and 6A<sub>g</sub> + 6A<sub>u</sub> librational lattice modes. Each internal vibration of the glycine and nondegenerate:  $\nu_1$  (A<sub>1</sub>) (= 1049 cm<sup>–1</sup>) and  $\nu_2$ (A<sub>2</sub>) (= 830 cm<sup>–1</sup>) nitrate ion vibrations should be split into two components being allowed either in IR (A<sub>u</sub>) or in Raman (A<sub>g</sub>) spectra, respectively. For the  $\nu_3$ (E') (= 1400 cm<sup>–1</sup>) and  $\nu_4$ (E') (= 720 cm<sup>–1</sup>) vibrations of the nitrate ion, the double degeneration is removed due to the C<sub>1</sub> site symmetry and each component is split into A<sub>u</sub> and A<sub>g</sub> modes due to the factor group coupling.

**Internal vibrations of the glycine molecule:** The powder IR and FT-Raman spectra of the  $\text{GLiNO}_3$  and its deuterated sample are shown in Figs. 3 and 4. The powder IR and FT-Raman spectra of the  $\text{GNaNO}_3$  crystal are shown in Fig. 5. The wave numbers of the bands and their tentative assignments are listed in Table 5 and Table 6.



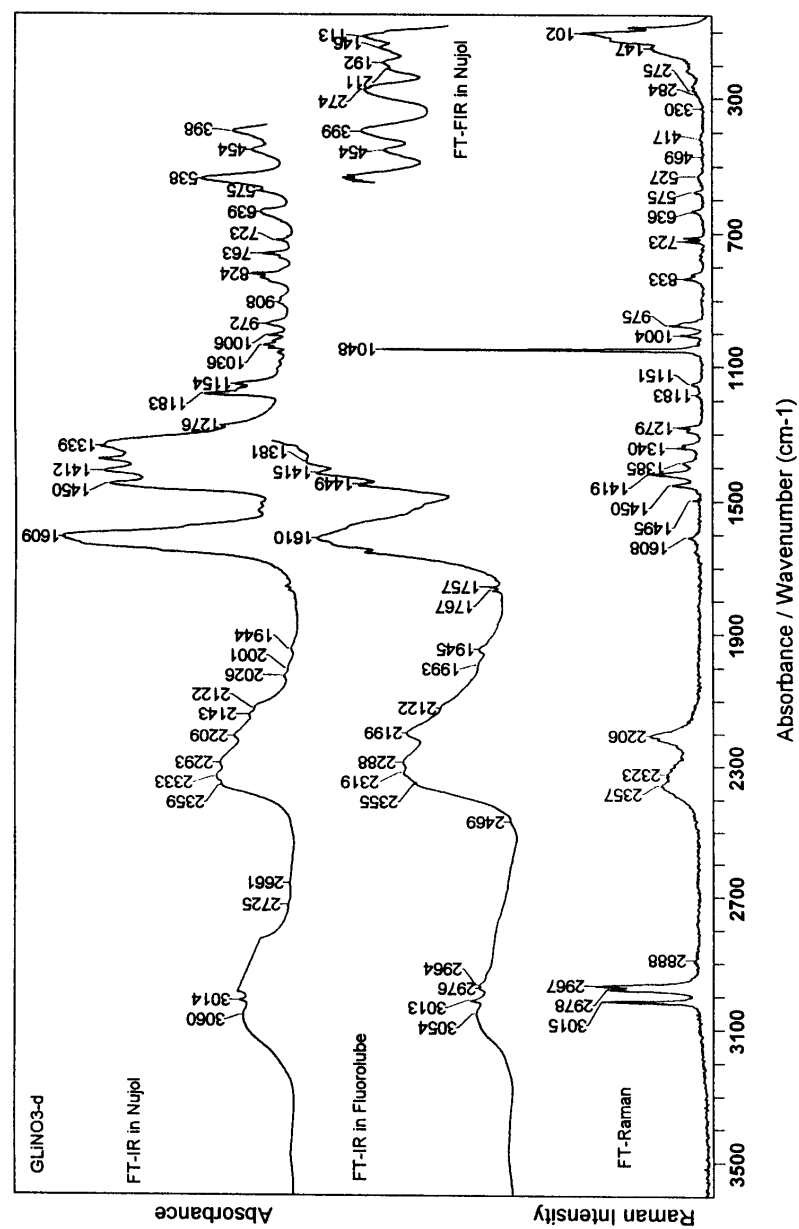


**Figure 4.** The powder IR (in Nujol and Fluorolube), FIR and FT-Raman spectra of the deuterated-GLiNO<sub>3</sub> sample.

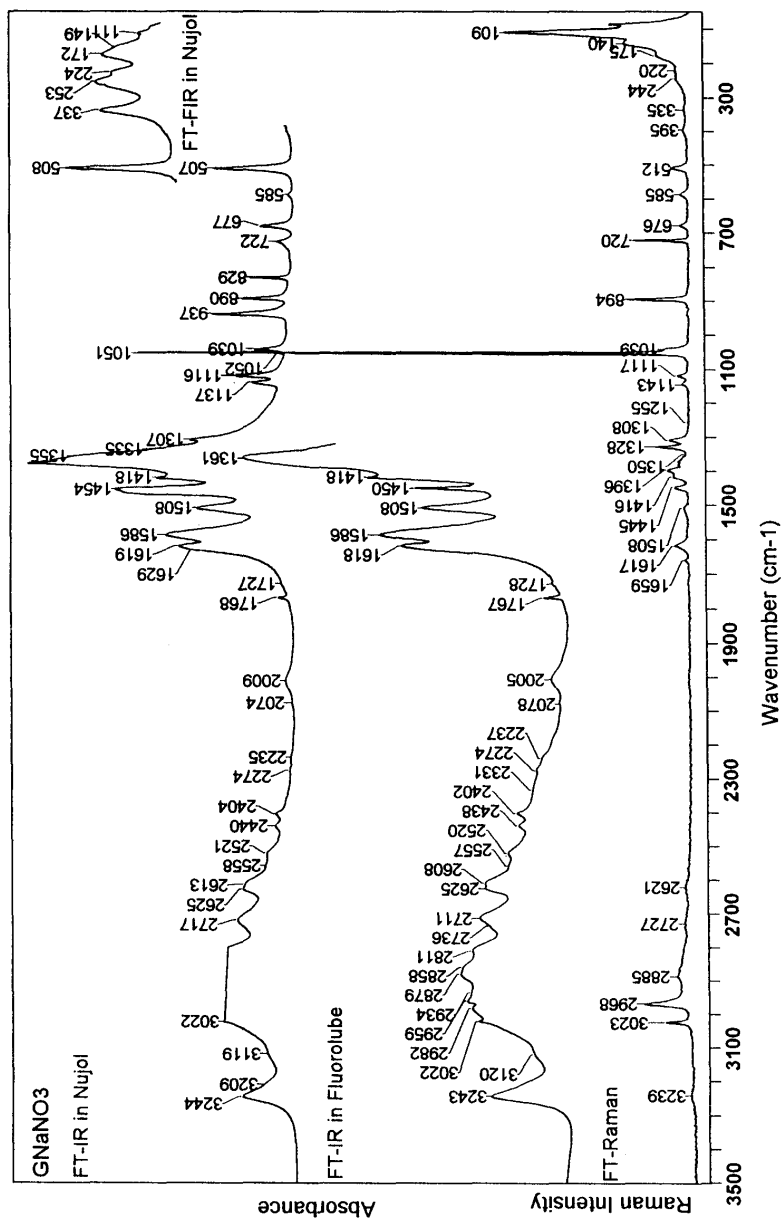


**Figure 5.** The powder IR (in Nujol and Fluorolube), FIR and FT-Raman spectra of the  $\text{GNaNO}_3$  crystal.

**Table 5.** Wavenumbers ( $\text{cm}^{-1}$ ), relative intensities ( $I_R^*$ ) and proposed assignments of the bands observed in the powder IR and FT-Raman spectra of the  $\text{GLiNO}_3$  and its deuterated analogue measured at room temperature.

GLiNO <sub>3</sub> -deuterated								GLiNO <sub>3</sub>				Assignment
In Nujol		Fluorolube		FT-Raman		In Nujol		Fluorolube		FT-Raman		
$\nu(\text{cm}^{-1})$	$I_R$	$\nu(\text{cm}^{-1})$	$I_R$	$\nu(\text{cm}^{-1})$	$I_R$	$\nu(\text{cm}^{-1})$	$I_R$	$\nu(\text{cm}^{-1})$	$I_R$	$\nu(\text{cm}^{-1})$	$I_R$	
3060	24	3054	27			3177	41	3180	28			$\nu\text{NH}\cdots\text{O}$
3014	26	3013	30	3015	30	3078	66	3066	52	3073	1	$\nu_a\text{NH}_3$
		2976	30	2978	30	3016	64	3016	49	3015	20	$\nu_a\text{CH}_2$
		2964	26	2967	38	2985	69			2978	30	$\nu_s\text{CH}_2$
								2961	48	2965	sh	$\nu_s\text{CH}_2$
								2935	47			$\nu_s\text{NH}_3$
										2907	1	
2725	6							2830	34			
2661	5					2726	19	2725	27			Overtone
						2623	16	2614	25			Overtone
						2537	7	2532	20			Overtone
						2512	19	2512	19			Overtone
						2491	19	2491	19			Overtone
		2469	13			2422	6	2419	20			Overtone
						2395	19	2395	19			
						2381	19	2381	19			
						2361	3	2348	19			
2359	33	2355	52	2357	15							$\nu_a\text{ND}_3$
2333	35			2323	15							$\nu_a\text{ND}_3$
		2319	57			2318	20	2318	20			
2293	34	2288	57									
						2279	18	2279	18			
						2215	15	2215	15			
2209	28	2199	56	2206	15							$\nu_s\text{ND}_3$
2143	22	2122	42									
2122	20	1993	27					2126	11			
2026	7											Overtone
2001	6					2007	1	2009	10			Overtone
1944	4	1945	26									Overtone
1768	5	1767	20					1873	8			Overtone
								1784	9			
1755	6	1757	22			1767	5	1767	12			
						1757	6	1756	12			
1649	59	1650	72			1659	53	1659	53			
						1634	86	1639	85	1644	2	$\delta_a\text{NH}_3$
								1632	87			$\delta_a\text{NH}_3$
1626	93	1628	86			1620	81	1622	84	1618	2	
1609	99	1610	92	1608	5	1606	74	1608	77	1597	2	$\nu_a\text{COO}^-$
1577	48	1576	80									$\delta_a\text{NH}_3$
1525	18	1560	73			1527	77	1525	78			$\delta_s\text{NH}_3$
1506	17	1509	49	1495	3	1507	82	1505	87	1495	2	$\delta_s\text{NH}_3$
						1465	67	1450	61			
1450	80	1449	75	1450	10	1455	79			1456	8	$\delta\text{CH}_2$
1412	83	1415	92	1419	15	1411	81	1415	83	1420	10	$\nu_s\text{COO}^-$
								1411	90			
1377	85	1381	97	1385	5	1376	100	1374	97	1373	1	$\nu_3\text{NO}_3$
				1363	2	1366	87	1362	94	1352	3	$\nu_s\text{ND}_3$

Table 5 (continuation)

1351	77				1350	79	1349	93			$\omega\text{CH}_2$
1339	84	1342	100	1340	11		1333	100	1335	8	$\omega\text{CH}_2$
1330	82			1331	10	1334	78		1318	9	$\tau\text{CH}_2$
						1311	67				$\tau\text{CH}_2$
1276	32										
1183	40			1183	5						$\delta_a\text{ND}_3$
1169	26			1151	6						$\delta_s\text{ND}_3$
1154	27										
						1116	22		1120	7	$\rho\text{NH}_3$
1109	10					1107	36				$\rho\text{NH}_3$
1086	9										
1060	10				1058	6		1059	100		$\nu\text{CN}$ or $\nu_1\text{NO}_3$
1047	13			1048	100	1046	10		1048	30	$\nu_1\text{NO}_3$
1036	16					1038	31		1039	10	$\nu\text{CN}$
1025	12			1027	3				1031	11	$\nu\text{CN}$
1006	13			1004	8						$\nu\text{CN}$
972	15			975	10						
968	13			969	Sh						
919	7					920	25		920	Sh	
908	9					910	47		909	21	$\nu\text{CC}$
895	9					899	25		898	Sh	$\rho\text{CH}_2$
844	13										
834	17			833	8						$\nu_2\text{NO}_3$
824	19			821	5	825	19				$\nu_2\text{NO}_3$
						817	9				$\nu_2\text{NO}_3$
776	9			775	2						
763	16			762	2						
					744	2			730	5	$\nu_4\text{NO}_3$
723	10			723	7	722	11		720	7	$\nu_4\text{NO}_3$
712	6			712	7	712	3		713	4	$\nu_4\text{NO}_3$
668	8			668	1	667	19		670	4	$\delta\text{COO}^-$
639	17			636	sh						def $\text{COO}^-$
				632	4						
575	17			575	4	581	14		592	2	def $\text{COO}^-$
									582	1	
538	41			527	3	546	42		535	1	def $\text{COO}^-$
454	20					455	16				$\text{T Li}^+$
432	16			417	1						$\text{T Li}^+$
398	29					413	28				$\text{T Li}^+$
				330	1						$\delta\text{CCN}$
				284	1						
274	30			275	2	274	30				lattice
				261	4						modes
211	sh			215	4				225	13	lattice
						197	sh		197	6	modes
192	25					192	15				lattice
									163	13	modes
146	19			147	10	146	14				lattice
									132	25	modes
113	25			123	30	113	30		122	20	lattice
				102	40				104	24	modes
											lattice

\*Relative intensities of the bands are given with respect to the strongest band ( $I_R = 100$ ) in each spectrum.

**Table 6.** Wavenumbers ( $\text{cm}^{-1}$ ), relative intensity<sup>\*</sup> and tentative assignment of the bands observed in the powder FT-Raman and IR spectra of the  $\text{GNaNO}_3$  crystal measured at room temperature.

FT-Raman		IR spectra				Tentative assignment
$\nu(\text{cm}^{-1})$	$I_R$	Nujol		Fluorolube		
		$\nu(\text{cm}^{-1})$	$I_R$	$\nu(\text{cm}^{-1})$	$I_R$	
3241	1	3244	50	3243	42	$\nu\text{NH}(\text{H}1\text{c})\cdots\text{O}(4\text{c})$
		3117	30	3116	25	$\nu\text{NH}\cdots\text{O}$
3023	5	3020	60	3022	43	$\nu_a\text{CH}_2$
				2982	40	
2969	8			2959	50	$\nu_s\text{CH}_2$
				2934	48	$\nu\text{NH}\cdots\text{O}$
2885	3			2879	53	$\nu\text{NH}\cdots\text{O}$
2863	2			2857	54	$\nu\text{NH}\cdots\text{O}$
2820	2			2810	47	$\nu\text{NH}\cdots\text{O}$
2723	2			2739	Sh	
		2717	60	2711	49	Overtone
2621	1	2625	50	2624	46	Overtone
		2609	55	2608	46	Overtone
				2557	39	Overtone
2532	1	2524	33	2520	39	Overtone
2437	1	2440	33	2438	29	Overtone
		2404	30	2402	30	Overtone
		2274	11	2272	25	Overtone
		2235	12	2234	sh	Overtone
				2189	10	Overtone
				2084	10	
2007	1	2009	11	2005	15	
		1768	23	1767	15	
1722	1			1727	12	
1658	1					$\delta_a\text{NH}_3$
1616	3	1619	83	1618	64	$\delta_a\text{NH}_3$
		1586	84	1586	70	$\nu_a\text{COO}^-$
1509	1	1508	73	1508	62	$\delta_s\text{NH}_3$
1447	3	1454	90	1450	62	$\delta\text{CH}_2$
1415	3	1418	80	1418	72	$\nu_s\text{COO}^-$
1396	4					$\nu_3\text{NO}_3$
1380	2					$\nu_3\text{NO}_3$
1370	2	1361	100	1361	99	$\nu_3\text{NO}_3$
1328	6					$\omega\text{CH}_2$
1308	4	1308	80			$\tau\text{CH}_2$
		1228	41			
		1169	33			$\rho\text{NN}_3^+$
1142	2	1137	44			$\rho\text{NN}_3^+$
1117	2	1116	53			$\rho\text{NN}_3^+$
1051	100	1051	22			$\nu_1\text{NO}_3$
1039	4	1039	44			$\nu\text{CN}$
		972	10			
952	0					
936	1	937	70			
932	1			917	22	
				890	55	$\rho\text{CH}_2$
895	11			829	51	$\nu\text{CC}$
870	1					$\nu_2\text{NO}_3$

Table 6 (continuation)

		771	11	
		735	12	$\nu_4\text{NO}_3$
720	10	722	13	$\nu_4\text{NO}_3$
676	2	677	40	$\delta\text{COO}^-$
585	2	585	11	$\text{def COO}^-$
507	3	507	72	$\text{def COO}^-$
398	1			
330	1	337	62	$\text{def CCN}$
		265	sh	
		253	60	
245	2			lattice modes
238	2			lattice modes
		224	sh	lattice modes
219	2			lattice modes
176	6	172	32	lattice modes
138	12	149		lattice modes
109	34	111	23	lattice modes
85	14			

\*Relative intensities are given with respect to the strongest band ( $I_R = 100$ ) in each spectrum.

The internal vibrations of the glycine molecules may be analysed taking into account the vibrations of the functional groups ( $\text{NN}_3^+$ ,  $\text{CH}_2$ ,  $\text{COO}^-$ ) and of the skeleton (CCN). They should be similar to those observed in the spectra of glycine crystals [8–18].

The stretching and bending vibrations of the  $\text{NH}_3$  group may be considered as vibrations of the  $\text{N}-\text{H}\cdots\text{O}$  hydrogen bonds. At first sight, the spectra of the GLiN and GNaN crystals seem to be similar. However, careful analysis clearly shows many differences, which can be related to differences in crystal structure of both these crystals. In the IR spectrum of the  $\text{GLiNO}_3$  crystal one can notice a broad band at  $3070\text{ cm}^{-1}$ , asymmetric from the low wave numbers region with additional structure and a shoulder at *ca.*  $3200\text{ cm}^{-1}$ . For such  $\text{N}-\text{H}\cdots\text{O}$  hydrogen bonds as those in the GLiN crystal one may expect the  $\nu\text{NH}$  bands close to  $3100\text{ cm}^{-1}$  according to the Nakamoto correlation [19]. As the  $\text{N}-\text{H}\cdots\text{O}$  hydrogen bonds in the  $\text{GLiNO}_3$  crystal are similar ( $2.8986(12)$ – $2.9343(13)$  Å; the N(1)–H(3) is involved in the bifurcated hydrogen bonds with the N···O distances  $2.8986(12)$  and  $3.1050(12)$  Å), therefore, the vibrations of the  $\text{NH}_3$  group may be considered as asymmetric ( $\nu_{\text{as}}\text{NH}_3$ ) and symmetric ( $\nu_{\text{s}}\text{NH}_3$ ) stretching observed at  $3070$  and at *ca.*  $2935\text{ cm}^{-1}$ , respectively. The other low frequency bands (till *ca.*  $2000\text{ cm}^{-1}$ ) are typical for the  $\text{N}-\text{H}\cdots\text{O}$  hydrogen bonds; they arise from the overtones. The IR spectrum of the GNaN $\text{O}_3$  is different from that of the GLiN crystal in this region, where a very strong and sharp band appears at  $3243\text{ cm}^{-1}$ . This can be due to the fact that one proton (H1c) of the  $\text{NH}_3^+$  group is involved in relatively weak hydrogen bond (N(1)–H(1c)–O(4c),  $2.893(4)$  Å) with respect to other two hydrogen bonds (N(1)–H(1a)···O(1<sup>i</sup>),  $2.789(4)$  Å; and N(1)–H(1b)···O(2<sup>ii</sup>),  $2.780(3)$  Å) [6].

It is surprising that the  $\nu_{\text{NH}}$  band of the highest wave number ( $3243 \text{ cm}^{-1}$ ) appears in the spectra of the GNan crystal instead of in the spectra ( $3180 \text{ cm}^{-1}$ ) of GLiN crystal. This is in contradiction to the fact that the hydrogen bonds are stronger in the GNan crystal ( $\text{N}(1)-\text{H}(1\text{a})\cdots\text{O}(1\text{a})$ ;  $2.789 \text{ \AA}$ , angle  $\text{NHO} 142.4^\circ$ ;  $\text{N}(1)-\text{H}(1\text{b})\cdots\text{O}(2\text{c})$ ,  $2.781 \text{ \AA}$ ,  $\text{NHO}$  angle  $150.9^\circ$ ;  $\text{N}(1)-\text{H}(1\text{c})-\text{O}(4\text{c})$ ,  $2.893 \text{ \AA}$ ,  $\text{NHO}$  angle  $154.9^\circ$ ) than those in the GLiN crystal ( $2.8986(12)$ ,  $3.1050(12)$ ,  $2.9343(13)$ ,  $2.9147(10) \text{ \AA}$ ). The presence of strong  $\text{NH}\cdots\text{O}$  bonds in the  $\text{GNano}_3$  crystal follows from the presence of strong bands in the region between  $3000$ – $2810 \text{ cm}^{-1}$ . Such conclusion follows also from analysis of the deformation vibrations of the  $\text{NH}_3^+$  observed in the region between  $1650$ – $1500 \text{ cm}^{-1}$  ( $\delta\text{NH}_3^+$ ) and in the region  $1140$ – $1100 \text{ cm}^{-1}$  ( $\rho\text{NH}_3^+$ ). Thus, in the case of the GLiN spectrum three bands appear at  $1658$ ,  $1632$ , and  $1507 \text{ cm}^{-1}$  and shoulders ( $1620$ ,  $1606$ ,  $1527 \text{ cm}^{-1}$ ) are observed. In the spectrum of the deuterated GLiN sample the strongest band remains at *ca.*  $1609 \text{ cm}^{-1}$ , whereas the other bands loose intensity. Its counterpart is observed at  $1608 \text{ cm}^{-1}$  with a low intensity in the Raman spectrum of the deuterated sample. This band arises from the asymmetric stretching vibration of the  $\text{COO}^-$  group. The IR spectrum of the GNan is much simpler in this region. Only three bands at  $1618$ ,  $1586$  ( $\nu_a\text{COO}^-$ ) and at  $1508 \text{ cm}^{-1}$  are observed in this region. It is a great surprise that this spectrum is so simple in this region. The region of rocking vibration of the  $\text{NH}_3$  group exhibits also well shaped and separated bands at  $1137$  and  $1117 \text{ cm}^{-1}$  in the case of GNan, whereas there is a very strong band at  $1106 \text{ cm}^{-1}$  with shoulder at  $1116 \text{ cm}^{-1}$  in the case of GLiN. The higher positions of these bands in the case of the GNan crystal may be explained by the stronger  $\text{NH}\cdots\text{O}$  hydrogen bonds than in the case of GLiN.

The symmetric stretching  $\nu_s\text{COO}^-$  modes in both crystals appear at very close wave numbers; namely at  $1411 \text{ cm}^{-1}$  in GLiN and at  $1418 \text{ cm}^{-1}$  in the GNan. The deformation vibrations of the  $\text{COO}^-$  appear at slightly higher wave numbers ( $677 \text{ cm}^{-1}$ ,  $585 \text{ cm}^{-1}$ ,  $507 \text{ cm}^{-1}$ ) in the case of GNan than that ( $662\text{sh}$  and  $668 \text{ cm}^{-1}$ ,  $581 \text{ cm}^{-1}$ ) of GLiN. The analogue of the  $507 \text{ cm}^{-1}$  band in the  $\text{GNano}_3$  is much stronger and appears at higher wave number ( $546 \text{ cm}^{-1}$  in IR and at  $535 \text{ cm}^{-1}$  in Raman) in the spectra of GLiN.

Among the vibrations of the  $\text{CH}_2$  group, only the scissoring vibration of the  $\text{CH}_2$  appears at the same wave number ( $1450 \text{ cm}^{-1}$ ) in both crystals. The other vibrations exhibit considerable differences. Thus, the  $\nu_a\text{CH}_2$  and  $\nu_s\text{CH}_2$  appear at  $3015$  and  $2978 \text{ cm}^{-1}$  ( $2965\text{sh}$ ) in the Raman spectrum of GLiN, whereas at  $3023$  and  $2969 \text{ cm}^{-1}$  in the case of  $\text{GNano}_3$ . The shoulder at *ca.*  $2965 \text{ cm}^{-1}$  in the case of GLiN changes into a strong band at  $2967 \text{ cm}^{-1}$  in the case of deuterated crystal. This splitting is observed both in Raman and IR spectra. The rocking  $\text{CH}_2$  vibration usually appears as a strong band in the IR and as a weak band in the Raman spectra and it is accompanied by the CC stretching vibration. Such condition is clearly obeyed in the spectra of the GNan crystal where these bands appear at  $890$  (w,  $\nu\text{CC}$ ) and  $937 \text{ cm}^{-1}$  (m,  $\rho\text{CH}_2$ ) in the IR and at  $895\text{w}$  and  $932 \text{ (vw) cm}^{-1}$  in the Raman spectrum. In the case of GLiN these two modes coincide in the IR spectrum giving a very strong band at  $910 \text{ cm}^{-1}$  with shoulders at *ca.*  $899$  and at  $920 \text{ cm}^{-1}$ . In the powder Raman spectrum there is a weak band at  $909 \text{ cm}^{-1}$  with shoulders at *ca.*  $898$  and  $920 \text{ cm}^{-1}$ . This observation

allows to assign the bands at *ca.* 910  $\text{cm}^{-1}$  to the  $\nu\text{CC}$ , whereas the shoulder to the  $\rho\text{CH}_2$ . The twisting and wagging modes of the  $\text{CH}_2$  are superimposed with the asymmetric stretching vibration ( $\nu_3$ ) of the  $\text{NO}_3$  ion. The bands at 1311 and 1334  $\text{cm}^{-1}$  in the IR spectrum may arise from the  $\tau\text{CH}_2$  and  $\omega\text{CH}_2$ , respectively, as their counterparts are also observed in the Raman spectrum. The other bands in this region are due to the  $\nu_3\text{NO}_3$  modes.

**Internal vibrations of the nitrate ions.** It is characteristic that all modes arising from the internal vibrations of the nitrate anion are split into a few components in the spectra of GLiN crystal. As the  $\text{NO}_3^{1-}$  anions occupy the  $\text{C}_1$  site, a splitting is expected for the  $\nu_3\text{NO}_3$  (1350, 1366, 1376  $\text{cm}^{-1}$  in IR and at 1373, 1352  $\text{cm}^{-1}$  in Raman) and for the  $\nu_4\text{NO}_3$  (730, 720, 713  $\text{cm}^{-1}$  in Raman) double degenerate modes [20]. However, no splitting is expected for the non-degenerate  $\nu_2\text{NO}_3$  (825, 817  $\text{cm}^{-1}$  in IR) and for the  $\nu_1\text{NO}_3$  (1059, 1048  $\text{cm}^{-1}$  in Raman and at 1059, 1048  $\text{cm}^{-1}$  in IR) modes. Such splitting is not observed in the case of GNan crystal. In the case of GNan crystal, a single band appears at 1051  $\text{cm}^{-1}$  in the Raman (very strong) and in the IR (very weak) spectra in the region of symmetric vibration  $\nu_1(\text{A}_1')$  of the  $\text{NO}_3$  ion. However, in the case of GLiN crystal two weak bands at 1058  $\text{cm}^{-1}$  and 1046  $\text{cm}^{-1}$  (shoulder) appear in the IR spectrum and also two bands at 1059  $\text{cm}^{-1}$  (very strong) and at 1048  $\text{cm}^{-1}$  (strong) appear in the Raman spectrum. This observation may suggest that these two bands are due to a dynamical splitting ( $\text{A}_u + \text{A}_g$ ) of the  $\nu_1\text{NO}_3$  mode. As both these modes are simultaneously active in Raman and in IR spectra, therefore, one may suggest that the space group of the crystal is  $\text{P}1$  instead of  $\text{P}\bar{1}$  as follows from the X-ray diffraction data. It is a surprise that the strongest Raman band at 1059  $\text{cm}^{-1}$  disappears on deuteration and only the band at 1048  $\text{cm}^{-1}$  remains. This can be explained assuming that the band at 1059  $\text{cm}^{-1}$  arises from the mode which is in fact in-phase ( $\text{A}_g$ ?) coupling between the  $\nu\text{CN}$  vibrations of the molecules in a dimer. This mode is not „pure” stretching vibration of CN bond only, but it is partly mixed with the deformation vibrations of the  $\text{NH}_3$  group [10–18]. Therefore, on deuteration this band disappears. For the second nondegenerate  $\nu_2\text{NO}_3$  (825, 817  $\text{cm}^{-1}$  in IR) vibration the splitting is clear as only the bands of the  $\text{NO}_3^{1-}$  appear in this region. In the case of deuterated crystal the bands of the  $\text{ND}_3$  rocking may appear in this region. This complicates the discussion.

**Translational modes of the lithium cations and lattice vibrations:** The bands at 455 and 413  $\text{cm}^{-1}$  observed only in the IR spectra arise from the translational vibrations of the  $\text{Li}^+$  cations with respect to the nitrate ions and oxygen atoms of the glycine zwitterions [21]. Their analogues are not observed in the spectra of the GNan crystal. It is possible that the lithium cations participate also in the mode at 538  $\text{cm}^{-1}$ . The analogue of this band appears at 507  $\text{cm}^{-1}$  in the case of the GNan crystal. The other bands observed below 300  $\text{cm}^{-1}$  arise from the deformation vibrations of the glycine skeleton and other lattice vibrations.

## CONCLUSIONS

The crystal structure of the Glycine-LiNO<sub>3</sub> complex has been determined at room temperature. It belongs to the centrosymmetric  $\bar{P}1$  space group of the triclinic system. Its structure is different from that of the Glycine-NaNO<sub>3</sub> analogue, which belongs to the polar Cc space group of the monoclinic system. The structure of the GNaNO<sub>3</sub> is built of layers formed by the Na<sup>+</sup> and NO<sub>3</sub><sup>1-</sup> ions and of the layers of the glycine zwitterions. In the case of GLiN crystal the lithium cations appear as centrosymmetric dimers, which are surrounded by six oxygen atoms (Li<sub>2</sub>O<sub>6</sub>) forming double tetrahedrons with a common edge. The double tetrahedrons seem to be the most important structural element in the GLiN crystal. The Li–O distances are between 1.9380(11) and 1.9974(12) Å. These distances correspond to those found in LiHCOO·H<sub>2</sub>O (1.923(4)–1.974(4) Å) [22], LiNH<sub>3</sub>SO<sub>4</sub> (1.939(6)–1.981(5) Å) [23] and LiH<sub>2</sub>PO<sub>3</sub> (1.922(5)–2.032(5) Å) [24]. The centrosymmetric dimers of the glycine molecules appear in the crystal. The assignment of the bands observed in powder IR and FT-Raman spectra is proposed and discussed with respect to the X-ray crystal structures. The CC stretching vibrations appear at different wave numbers in both these crystals. This is in agreement with the crystal structure, where the CC bond is shorter in the GLiNO<sub>3</sub> (1.5169(8) Å) than that (1.520(4) Å) in the GNaNO<sub>3</sub> [6].

The differences in the structure and strength of the N–H···O hydrogen bonds in both these crystals are also clearly seen in the vibrational spectra. A splitting of some bands arising from internal vibrations of the nitrate anion and also from the  $\nu_s$ CH<sub>2</sub> observed in the spectra of the GLiNO<sub>3</sub> crystal may suggest lower space group symmetry (P1) than that  $\bar{P}1$  determined by the X-ray diffraction experiment. Therefore, the crystal structure was examined for P1 and for  $\bar{P}1$  space group. Refinement unequivocally indicated that the crystal structure was centrosymmetric; space group  $\bar{P}1$ .

**Supplementary material.** Crystallographic data for structure reported in this paper have been deposited at Cambridge Crystallographic Data Centre as supplementary publication number CCDC 209183. These data can be obtained free of charge *via* [www.ccdc.com.ac.uk/conts/retrieving.html](http://www.ccdc.com.ac.uk/conts/retrieving.html) (or from the Cambridge Crystallographic Data Center, 12 Union Road, Cambridge CB2 1EZ, UK; fax: +44 1223 336033; or [deposit@ccdc.com.ac.uk](mailto:deposit@ccdc.com.ac.uk)).

## Acknowledgments

The authors acknowledge the financial support by the Polish State Committee for Scientific Research (KBN project No. 7 T09A 014 20).

## REFERENCES

1. Pepinsky R., Okaya Y., Eastman D.P. and Mitsui T., *Phys. Rev.*, **107**, 1538 (1957).
2. Pepinsky R., Vedam K. and Okaya Y., *Phys. Rev.*, **110**(6), 1309 (1958).
3. Pepinsky R. and Makita Y., *Bull. Amer. Phys. Soc. Series II*, **7**, 241 (1962).
4. Narayan Bhat N. and Dharmaprakash S.M., *J. Cryst. Growth*, **235**, 511 (2002).
5. Sheldrick G.M., SHELX-97 Programs for refinement of crystal structures.

6. Krishnakumar R.V., Subha Nadhimi M., Natarajan S., Sivakumar K. and Varghese B., *Acta Cryst.*, **C57**, 1149 (2001).
7. Perlovich G.L., Hansen L.K. and Bauer-Brandl A., *J. Thermal Analysis and Calorimetry*, **66**, 699 (2001).
8. Steinback H., *J. Raman Spectrosc.*, **5**, 49 (1976).
9. Krishnan R.S. and Narayanan P.S., *Crystallography and Crystal Perfection*; Proceedings of a Symposium held in Madras 14–18 January 1963. Edited by G.N. Ramachandran, Academic Press, London and New York, 1963, pages 329–346.
10. Rosado M.T., Duarte M.L.T.S. and Fausto R., *Vib. Spectrosc.*, **16**, 35 (1998).
11. Williams R.W., Kalasinsky V.F. and Lowrey A.H., *J. Mol. Struct.(Theochem)*, **281**, 157 (1993).
12. Machida K., Kagayama A., Saito Y., Kuroda Y. and Uno T., *Spectrochim. Acta*, **33A**, 569 (1977).
13. Machida K., Kagayama A. and Saito Y., *J. Raman Spectrosc.*, **8**, 133 (1979).
14. Machida K., Mori M., Kagayama A. and Saito Y., *J. Raman Spectrosc.*, **9**, 139 (1980).
15. Kharina R.K., Horak H. and Lippincott E.R., *Spectrochim. Acta*, **22**, 1759 (1966).
16. Chakraborty D. and Manogaran S., *Chem. Phys. Lett.*, **294**, 56 (1998).
17. Alper J.S., Dothe H. and Lowe M.A., *Chem. Phys.*, **161**, 199 (1992).
18. Kakihana M., Akiyama M., Nagaumo T. and Okamoto M., *Z. Naturforsch.*, **43a**, 774 (1988).
19. Pimentel G.C. and McClellan A.L., *The Hydrogen Bond*, Freeman and Co., San Francisco, London, 1960, page 97.
20. Herzberg G., *Infrared and Raman Spectra of Polyatomic Molecules*, D. Van Nostrand Company, Inc., NY, 1945, page 178.
21. Vierne R. and Cadene M., *Ferroelectrics*, **5**, 91 (1973).
22. Enders-Beumer A. and Harkema S., *Acta Cryst.*, **B29**, 682 (1973).
23. Vilminot S., Anderson M.R. and Brown I.D., *Acta Cryst.*, **B29**, 2628 (1973).
24. Johansson G.B. and Lindqvist O., *Acta Cryst.*, **B32**, 412 (1976).